

## iSIMM looks beneath basalt for both industry and university research

Philip Christie\* (Schlumberger Cambridge Research), Andrew Langridge (WesternGeco), Robert White, Zoë Lunnon, Alan W. Roberts (Cambridge University) and the iSIMM team†.

### Summary

The integrated Seismic Imaging and Modelling of Margins (iSIMM) project is a joint industry-university research project seeking to characterise magmatic ocean margins and to develop new models for their evolution. In summer 2002, seismic data were acquired successfully over two such margins: the Hatton-Rockall margin and the margin to the northeast of the Faroe Islands, using a combination of towed streamers and Ocean-Bottom Seismometers (OBS). This paper focuses on the profile acquired over the Faroe margin, where a 385 km profile was acquired by Cambridge University with OBS and by WesternGeco with three single-sensor streamers, each using a source array tuned for low frequencies. Both techniques seek to image beneath the basalt cover and, through their integration, to develop a structural model from the seabed to the Moho. This will constrain new theoretical models which address the development of rifted continental margins, including the effects of dynamic support by mantle plumes and the production and intrusion of igneous melt.

### Introduction

The early Tertiary onset of seafloor spreading in the North Atlantic was accompanied by extensive magmatism, believed to be caused by the interaction of the Iceland mantle plume with lithospheric rifting (Barton & White, 1997). In contrast to other margins which display little magmatism, much of the North Atlantic is characterised by massive lava flows extending away from the rifted margin across the hydrocarbon-prospective basins on the Atlantic margin (e.g., Richardson et al. 1999). The extruded material appears to be accompanied, in places, by intrusion of sills into the sedimentary sequence, lower-crustal sill intrusion and/or igneous underplating. This resulted in permanent uplift in the affected areas.

The magmatism provides a challenge both to imaging basin structure, and to modelling the subsidence and development of the continental margins. The iSIMM program integrates strategies for imaging and then modelling the effects of the extrusive lavas, sills and lower-crustal intrusions. Many of the imaging difficulties can be surmounted by using very long offsets (long streamers or two-ship methods) (White et al. 1999) with a low-frequency bandwidth source, and by using static OBS.

Combinations of new streamer, OBS, gravity and magnetometer data were acquired in two long transects across contrasting continental margins (Figure 1). The first transect crosses the Faroes-Shetland Trough, the

Faroes Shelf, the adjacent continental margin and oceanic crust (Figure 2), using coincident wide-angle OBS acquisition and long-offset, multi-streamer swaths. This margin displays both extensional and strike-slip components, and is close to the presumed mantle plume centre. The second transect, acquired with simultaneous OBS and standard-offset streamer data, crosses the Hatton-Rockall Basin, Hatton Bank and ends far onto the adjacent oceanic crust (Figure 1), in an area where previous work has shown there to be considerable underplating, sills in the sediments, and extensive lavas extruded close to sea level (Morgan et al. 1989). This margin is extensional, and is further from the mantle plume (Smallwood & White, 2002).

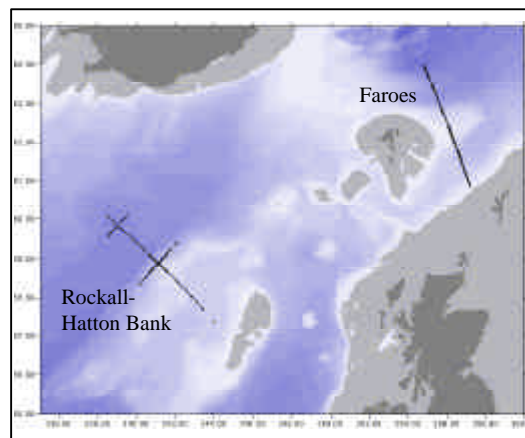


Figure 1: Locations of OBS laid across the Rockall-Hatton Bank margin and the Faroes margin by *RRS Discovery*.

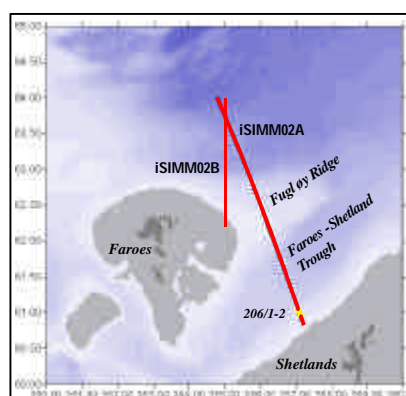


Figure 2: Long-offset, multi-streamer swaths acquired by *M/V Geco Topaz*. iSIMM02A overlies the OBS profile in Figure 1. iSIMM02B is a second transect of the margin shot by *Topaz* only.

\*Schlumberger Cambridge Research, High Cross, Madingley Road, Cambridge CB3 0EL, UK. pafc1@slb.com

† Roman Spitzer, Craig Parkin, Lindsey Smith, Nick Kusznir, Vijay Tymms, Neil Hurst and Alan Roberts

Both surveys extended from 120 km to 160 km over the adjacent oceanic crust, to measure igneous crustal thickness variations following the first 15 Ma after break-up: the plume temperature was pulsing on a 3 to 5 Ma timescale (White 1997), and the oceanic crustal thickness provides a sensitive thermometer of the mantle temperature. Such plume temperature variations are crucial in assessing the hydrocarbon potential of the adjacent basins because they cause rapid regional uplift and subsidence, and have been postulated to control sedimentation pulses (White & Lovell, 1997).

The deep waters of rifted continental margins are the frontier exploration areas for the hydrocarbon industry, and a sound understanding of the breakup process and the nature of the continent-ocean transition is of prime importance to oil industry exploration in these regions. However the recent discoveries of heterogeneous (depth-dependent) stretching and mantle exhumation are not predicted by existing quantitative models of rifted margin formation, which are usually based on intra-continental rift models subjected to very large stretching factors. New quantitative models of rifted margin formation are being developed and tested as part of the iSIMM project. Two-phase flow models of mantle flow and melt transport, previously used successfully at ocean ridges, are being adapted to the initiation of seafloor spreading and the formation of rifted margins. The new quantitative model of rifted margin formation will also be used to model and predict subsidence and heat flow history at rifted margins for deep-water exploration.

In addition to addressing the general problem of magmatic margin evolution, the iSIMM project also seeks to evaluate seismic acquisition and processing technology to access sedimentary structures overlain by basalt flows. In the context of the Faroes profile (Figure 2), extending from sediments free from basalt in the south through increasing basalt cover to oceanic crust in the north, there is good circumstantial evidence for prospective hydrocarbon structures beneath the basalt carapace. In the UK sector of the Faroes-Shetland Trough, the oilfields of Foinaven and Schiehallion produce from turbiditic channel sands in the T31 to T34 age range (~60–58 Ma) (Cooper et al. 1999). The recently-discovered Marjun hydrocarbon accumulation, the first in Faroese waters, lies deeper in the Faroes-Shetland Trough section in earlier T10 sands (~64 Ma) (Smallwood et al. 2002). These reservoirs demonstrate the existence of source rocks, reservoir rocks and seals that pre-date the Faroes basalts which were extruded in the interval 59 to 55.5 Ma (Andersen et al. 2002). Although it must be noted that no discovery has yet been drilled beneath basalt in the Faroes, the circumstantial evidence motivates the exploration for hydrocarbon beneath the basalt.

### Generating low frequencies

A sequence of sub-aerially emplaced basalt flows is highly heterogeneous. The boundaries of each flow are characterised by a shift to lower velocities and density, caused by the formation of vesicles at the top and base of the flow (Planke & Cambray 1998), and by weathering and alteration. The heterogeneity causes spectral colouration and scattering loss in seismic transmission. Where the flow boundaries are also rough, there is further scattering loss. However, Dancer & Pillar (2002) described the use of low-frequency seismic energy to image the gas-bearing sands of the Corrib field, west of Ireland, which are overlain by shallow basalts. Mack (1997) modelled the effects of layered basalt flows and proposed the use of low frequencies to minimise scattering loss. Christie et al. (2002 and in press) estimated scattering loss of 35 in layered basalts from a VSP in the Lopra 1/1A borehole, which penetrated some 3,600 m of Lower Series basalt flows, and tied the VSP to a synthetic seismogram created from sonic and density log data. Ziolkowski et al. (2001) also proposed the use of low frequencies for sub-basalt imaging and suggested the use of large airguns towed deep to generate the low-frequency bandwidth. In the towed streamer and OBS acquisitions along the Faroes profile, low frequencies were produced by adapting the bubble-tuned airgun method proposed by Avedik (1993). To allow a comparison, the OBS profile was also shot using the same airgun array with conventional peak tuning (Lunnon et al. 2003).

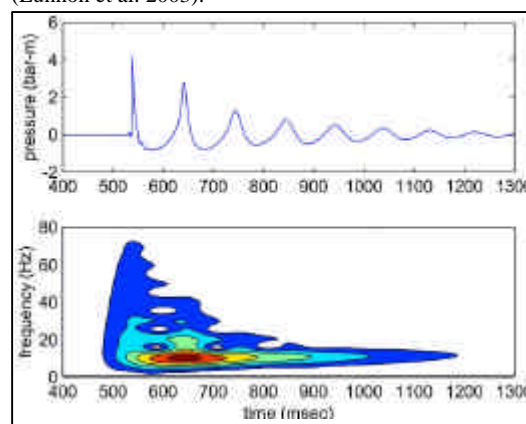


Figure 3: Free-field signature (upper) and frequency-time plot (lower) of a 400 in<sup>3</sup> airgun, fired at 10 m depth. Contour interval 20 dB with warm colours denoting high amplitudes.

The free-field signature of a 400 in<sup>3</sup> airgun, fired at 10 m depth with no free-surface reflection, is displayed in Figure 3. The primary pulse is followed by a sequence of reverberations, caused by bubble oscillations in the water. The bubble period is described by the Rayleigh-Willis relation and predicts an increase in period with increasing gun volume and a decrease in period with increasing depth. A frequency-time analysis, created by computing the spectrum inside a running Gaussian

window of half-width 107 ms, is also shown in Figure 3. The highest frequency bandwidth is at the front of the signature coinciding with the primary pulse. However, the highest amplitude occurs at about 10 Hz, coinciding with the first bubble at 640 ms.

Conventional airgun arrays use guns with a variety of volumes fired simultaneously to enhance the primary pulse and to minimise the bubble reverberation by destructive interference, producing a signature rich in high frequency bandwidth. A bubble-tuned array staggers the gun firing with delays that increase with decreasing gun volume, so as to align the first bubbles and emit a signature rich in low frequency bandwidth.

The reflected signal, or ghost, from the free-surface above an airgun suffers a reversal in phase and interferes with the downgoing primary signature. At distances far compared to the depth of the gun, the free-field signature is effectively convolved with a dipole operator (1,-1) where the dipole elements are separated by a time equal to the delay between the primary and the ghost. This delay,  $\Delta t$ , varies with take-off angle,  $\theta$ , from the vertical according to the relation:

$$\Delta t = 2d \cdot \cos \theta / v$$

where  $d$  is the depth of immersion of the gun and  $v$  is the velocity of sound in water. The dipole operator colours the free-field spectrum of the signature (Figure 4) enhancing a bandwidth of 2.32 octaves about the frequency for which the depth is a quarter-wavelength, at which the relative amplitude peaks at 2 (constructive interference). At 0 Hz and at multiples of the ghost-notch frequency, corresponding to a half-wavelength depth of immersion, the dipole operator has a zero corresponding to destructive interference. The operator is replicated at multiples of the ghost notch but only the base band is shown for simplicity. There is, of course, a similar effect for the streamer ghost.

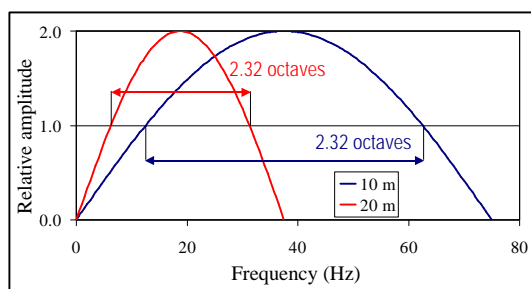


Figure 4: Ghost notch spectra for guns at 10 m and 20 m depths.

Increasing the depth of immersion decreases the frequency of peak enhancement, and the octave bandwidth of enhancement is the same whatever the depth of immersion. However, increasing the ambient pressure on the bubble released from the gun decreases the bubble period, following Rayleigh-Willis, so there is

a trade-off in the two effects, resulting in an optimal depth for a given gun when bubble tuning (Avedik 1993). The iSIMM bubble-tuning approach differed from that of Avedik in using Bolt LL guns at a constant depth, instead of GI injector guns at varying depths. Constant depth facilitated the operations and the sources for both OBS and towed streamer acquisitions were designed for an optimal, low frequency signatures prior to the surveys (Lunnon et al. 2003).

### Comparison of peak and bubble tuning

The OBS profile across the Faroes margin was shot twice by the *RRS Discovery*, once with peak-tuning and a second time with bubble tuning. The source comprised four sub-arrays (with guns of 120, 160, 300, 400, 500 and 700 in<sup>3</sup>) at a constant 22 m depth, and two 1,000 in<sup>3</sup> guns towed at about 18 m depth. The source comprised 14 guns of total volume 6,360 in<sup>3</sup>, fired at 140 bar. Apart from the tuning method and sailing direction, all other source parameters were the same for the two passes. Far-field signatures were estimated at a few control points using vertical hydrophone arrays (VHA) which allowed separation of the up- and down-going wavefields in the water (Lunnon et al. 2003).

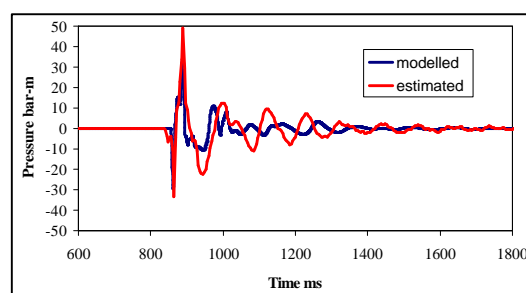


Figure 5a: Comparison of far-field signatures for the peak-tuned OBS source estimated from the VHA (red) and from pre-survey modelling (blue).

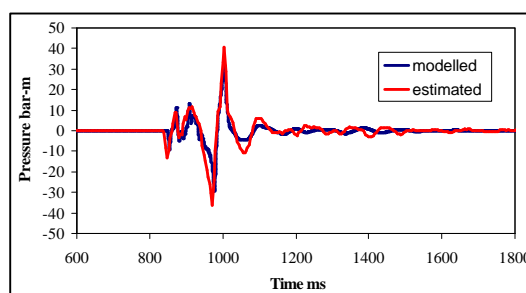


Figure 5b: Comparison of far-field signatures for the bubble-tuned OBS source estimated from the VHA (red) and from pre-survey modelling (blue).

Comparisons of pre-survey modelled signatures and signatures estimated from the VHA are shown in Figures 5a and 5b. In both cases the pre-survey modelling has under-predicted the estimated amplitudes of the actual

signatures by about 14%. While the modelled bubble-tuned signature is quite a good match to the estimated signature (Figure 5b), the peak-tuned model is a poor predictor of the estimated waveform (Figure 5a). The bubble-tuned signatures are quite compact, with a well-defined principal peak, but the estimated peak-tuned signature is rather reverberant, which was not predicted by the model.

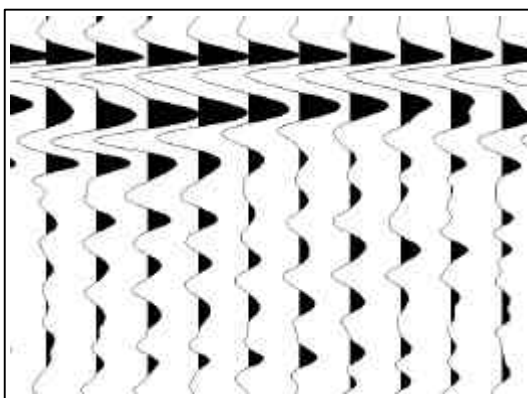


Figure 6a: Sample first arrival data from peak-tuned OBS section at about 30 km offset after linear moveout correction at 7 km/s. The arrivals have two peaks and a reverberatory tail which masks structure on the left half of the section. Offset increases to the right; the window extends 900 m in offset and 800 ms in TWT.

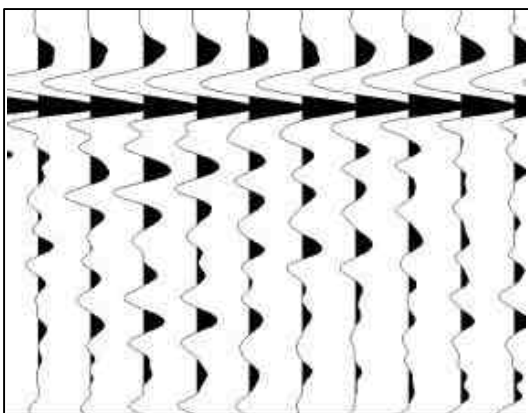


Figure 6b: Corresponding traces from bubble-tuned OBS section. The arrivals have a clear main peak and a compact tail which reveals structure following the first arrivals.

Figures 6a and 6b show sample OBS data from the same 30 km offsets for the peak- and bubble-tuned data, where much of the higher frequencies seen in the modelled and

estimated signatures in the water have been removed by the earth filter. At these offsets, the first arriving energy is a crustal arrival with an almost horizontal moveout following a linear moveout correction of 7 km/s. The peak-tuned traces (Figure 6a) have twin peaks and a reverberant tail, as seen on the estimated signature. The bubble-tuned data (Figure 6b) have a single main peak and less reverberation, allowing structure to be seen in the coda following the main arrival. Because OBS data analysis involves mode identification and traveltimes picking for inverse ray-tracing and subsequent forward modelling, picking quality is a key attribute. While both types of tuning have resulted in data sections showing good signal-to-noise ratio, suggesting that gun depth is more important than the method of tuning, the bubble-tuned data have an edge for the OBS analysis.

#### Faroes towed streamer acquisition

The *M/V Geco Topaz* acquired the towed streamer survey which overshot the same profile as that acquired earlier by the *RRS Discovery*. The *Topaz* towed three, single-sensor, streamers, two of 4 km and one of 12 km, in a swath to provide both long offsets and cross-line protection at shorter offsets. The streamers were towed at 18 m depth and the combination of deep tow, good weather and on-board digital group forming (Martin et al. 2000) provided data sampled at 12.5 m, with high signal-to-noise ratio.

A wide source was formed by combining two standard source arrays, also towed at 18 m depth and tuned on the first bubble. Since the time budget would allow just a single pass, it was decided to follow the OBS experience on *Discovery* and use bubble-tuning on the six identical sub-arrays. The source volume was 10,170 in<sup>3</sup> and was fired at 140 bar with a 50 m pop interval to acquire 18 s records. This would allow the acquisition of doubly-mode-converted shear events at long offsets which elsewhere have been used successfully to image beneath basalt (Emsley et al. 1998). Pre-survey modelling showed a benefit at low frequencies for the bubble-tuned source, although less of a benefit than for the case of the OBS source. Figure 7 shows three modelled source signatures after passing through a filter simulating the effect of two-way propagation through a 2 km basalt layer with an effective Q of 35. The traces have been time-aligned for ease of comparison. The red trace is the modelled peak-tuned signature; the blue trace is the modelled bubble-tuned signature and the green trace is a "conventional" signature from a 4,017 in<sup>3</sup> source towed at 8 m. Both the deep-towed source signatures have significantly higher low-frequency amplitudes than the standard source, with the bubble-tuned signature again having an edge.

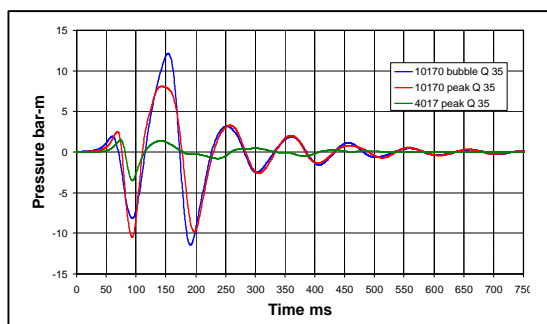


Figure 7: Comparison of pre-survey modelled signatures from the bubble-tuned source (blue), the peak-tuned source (red) and a conventional source (green) after two-way passage of a plane wave through 2 km of basalt with scattering loss modelled by an effective Q of 35.

The acquisition was carried out using the TRISOR on-board source controller which not only allowed the bubble tuning to be set up but also allowed acquisition of near-gun hydrophone traces for computation of a calibrated marine signature (CMS) using the Notional Source algorithm (Ziolkowski et al. 1982). On-board source evaluation showed that the CMS far-field signature was a good match to the pre-survey modelled signature and was very stable.

The long-offset seismic data have a good signal-to-noise ratio and events with linear moveout are seen at larger offsets. The OBS are spaced at 6 km over most of the profile, but a 50 km section has OBS spacing of 2 km, resulting in 2–7 OBS stations in every 12 km gather, which will facilitate correlation between the data types.

#### Towed Streamer Processing and Initial Results

The first processing of the 12 km streamer data was recently completed by the WesternGeco processing group in Gatwick. A key enabler for the use of the bubble-tuned source was the ability to estimate the far-field source signature on a shot-by-shot basis. Because of the staggered firing delays to the different gun elements, the signature is mixed phase. After convolution with the streamer ghost, an average source signature was estimated and a shot-by-shot shaping filter was applied to remove any residual source variation. At this point, detailed testing took place to determine the optimum working signature and bandwidth. Since conventional seismic is known to be effective in imaging the post-basalt sequence, it was decided to focus on the low-frequency bandwidth for sub-basalt penetration. Consequently, the source wavelet was whitened and shaped to a zero-phase wavelet in the band below the first ghost notch at about 42 Hz. Figure 8 shows the field signature convolved with a streamer ghost in comparison to the final shaped signature. Figure 9 shows the comparative spectra, where the shaped signature has also been high-cut filtered to attenuate energy above the first notch. This signature processing strategy has been

effective for the sub-critically reflected data. Wide-angle reflections, which are the subject of further research in the Cambridge group, have an alternative wavelet processing strategy because of the marked changes in phase near the critical angle.

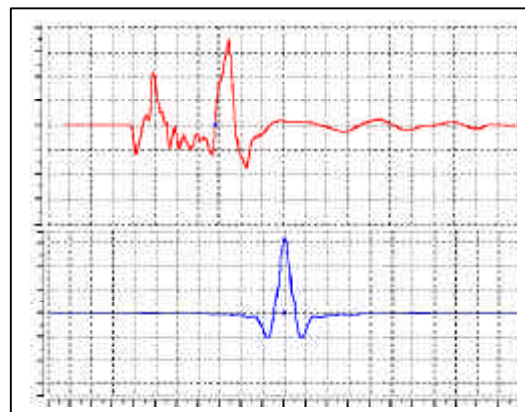


Figure 8: Comparison of field estimated signature convolved with the streamer ghost (upper, red), and the processing wavelet after designation (lower, blue). Timing lines are at 30 ms.

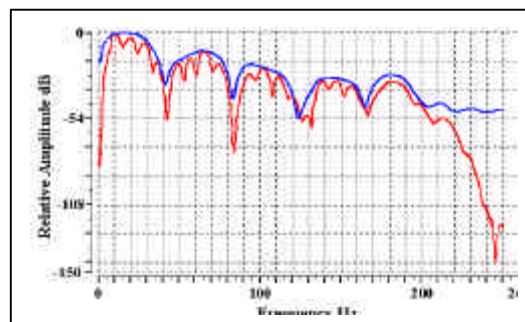


Figure 9: The spectra corresponding to the wavelets in Figure 8 where red is the field signature with streamer ghost and blue is the deconvolved wavelet. The shaping has whitened the spectrum. The first ghost notch is at 42 Hz and the useful sub-basalt bandwidth is below this frequency.

In sub-basalt imaging, the attenuation of long period multiples generated between the major impedance boundaries of free surface, sea-bed, top basalt and base basalt requires careful processing. The strategy combined a Kirchhoff wavefield inversion method with a moveout-dependent Radon transform method. For the former, the WesternGeco implementation of surface-related multiple elimination called Interbed Multiple Prediction was the preferred approach (e.g., see Dragoset 1999). Since the algorithm is not velocity-dependent, it was able to work effectively even when the sub-basalt velocity profile was uncertain. In this case it was used solely for water-column multiples, and worked best in attenuating multiple energy on the near offsets. In addition, two passes of Radon transform, in conjunction with multiple-trend velocity picking, were used to remove faster

multiples and remaining energy on the longer offsets. Prediction of the multiples generated by the top basalt horizon allowed picking of the second multiple trend.

Only at the pre-stacking stage, after a significant amount of multiple had already been removed, was a primary-retaining Radon transform applied. This used a velocity mute at 85% of the (now more confident) picked primary velocities. Fourth-order moveout was also adopted to flatten the farther offsets. True-offset CMP gathering was employed to accommodate the fairly significant feather angles on the 12 km cable.

Partial pre-stack migration was introduced at this stage to remove stacking conflicts and improve the primary velocity picking. This comprised a constant velocity (2,000 m/s) NMO, DMO and Stolt Migration. The migration was backed off post-stack, to allow a full Kirchhoff migration to be applied using a smoothed version of the primary velocity field. Careful angle muting at the top basalt, and outer and inner muting deeper in the section, were critical to the resolution of stacked events.

In Figure 10, a sample section is shown from the final migration which crosses the basalt escarpment on the northwestern flank of the Faroes-Shetland Trough. The window comprises some 25 km of data and extends to

about 5 s two-way time (TWT). Northwest is to the left of the image. Water depth at the left edge is about 690 m, deepening to 1390 m down the flank of the trough. The top of the basalt is at about 2700 ms at the left edge of the image and is probably just below the strong, smooth reflector seen here which itself may be the Balder ash marker. Between 3000 ms and 3700 ms, there is an interesting sequence of sigmoidal structures which may represent palaeo-shorelines of the basalt flows. Down-dip from this sigmoidal sequence is the subsurface basalt escarpment which has been identified and described by other authors (Kjørboe 1999).

The sigmoidal features are almost certainly below the top basalt and are indicative of structure internal to the basalt sequence. The base basalt is a matter of conjecture but there are horizons around 4100 ms and 4700 ms, either of which might be the base of the basalt flows, although the selection of the latter would infer a thickness in excess of 5 km, which is less likely. Further support will derive from detailed velocity analysis from the closely spaced OBS over the area in conjunction with the long-offset arrivals from the towed streamer data. Additionally, tomographic velocity analysis as part of a pre-stack depth migration may help to identify base basalt with greater confidence. Both approaches will be supported by analysis of the gravity data acquired by the *RRS Discovery* over the same profile.

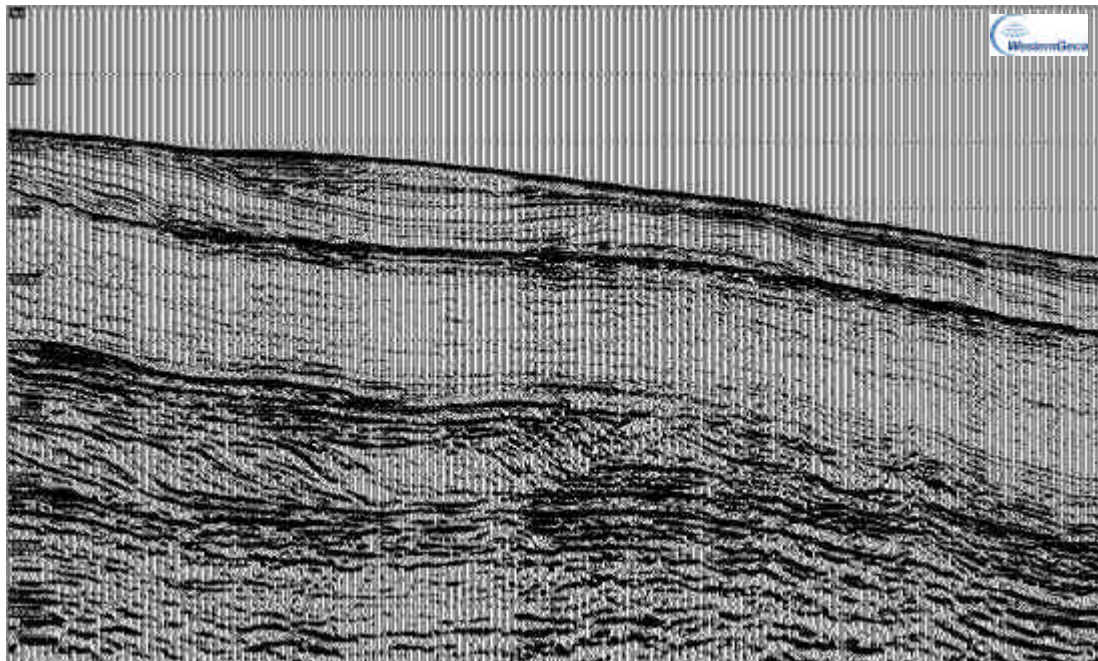


Figure 10: Sample section from the Faroes towed streamer profile. The window is about 25 km by 5 s TWT in extent, centred upon the basalt escarpment, with northwest to the left. The dotted timing lines are at 500 ms intervals. Clearly visible are the sigmoidal foresets updip of the escarpment, suggestive of a prograding basalt shoreline. *Courtesy WesternGeco.*

## Conclusions

In 2002, the iSIMM project acquired both towed streamer and OBS data over two North Atlantic margins in the Hatton-Rockall area and northeast of the Faroe Islands. One goal is to characterise magmatic margins and drive the development of models capable of simulating the spatio-temporal evolution of subsidence and heatflow. In the Faroes region a 385 km profile was shot with OBS and long-offset, single-sensor, Q\*-streamers, using sources designed for low frequencies. The OBS profile was shot twice to allow a comparison of peak and bubble tuning. Both sources gave good results, with the bubble-tuned source having a more compact, less reverberant signature to facilitate arrival picking for inverse traveltimes analysis. The streamer profile was also acquired using a bubble-tuned source which gave good penetration below the basalt top for sub-critical events revealing structure beneath the top basalt. Key aspects of the acquisition and processing included shot-by-shot signature monitoring allowing waveshaping, and careful demultiple. Further analysis, integrating the different data sources and focusing on the long-offset arrivals will help to identify the base of the basalts and illuminate deeper structure using wide-angle imaging techniques, such as those developed by Flidner and White (2001).

## References

- Andersen, M.S., Sørensen, A.B., Boldreel, L.O., and Nielsen, T., 2002, Cenozoic evolution of the Faroe Platform: comparing denudation and deposition. *In: Doré, A.G., Cartwright, J.A., Stoker, M.S., Turner, J.P., and White, N., (eds) Exhumation of the North Atlantic Margin: Timing, Mechanisms and Implications for Petroleum Exploration*, Special Publications, **196**, 291–311, Geological Society, London.
- Avedik, F., Renard, V., Allenou, J.P., and Morvan, B., 1993, Single bubble air-gun array for deep exploration. *Geophysics* **58**, 366–382.
- Barton, A.J., and White, R.S., 1997, Crustal structure of the Edoras Bank continental margin and mantle thermal anomalies beneath the North Atlantic. *Journal of Geophysical Research* **102**, 3109–3129.
- Christie, P.A.F., Gollifer, I., and Cowper, D., 2002, Borehole seismic results from the Lopra Deepening Project, *Journal of Conference Abstracts*, **7**(2), 138–139.
- Christie, P.A.F., Gollifer, I., and Cowper, D., Borehole seismic studies of a volcanic succession from the Lopra1/1A borehole in the Faroe Islands, NE Atlantic. *Geology of Denmark Survey*, in press.
- Cooper, M.M., Evans, A.C., Lynch, D.J., Neville, G., and Newley, T., 1999, The Foinaven Field: managing reservoir development uncertainty prior to start-up. *In: Fleet, A.J., & Boldy, S.A.R. (eds) Petroleum Geology of Northwest Europe: Proceedings of the 5<sup>th</sup> Conference*, 675–682, Geological Society of London.
- Dancer, P.N., and Pillar, N.W., 2002, Successful sub-basalt imaging with enhanced low frequency 3D seismic data: Corrib Field, West of Ireland, presented at: Frontier Exploration of Volcanic Continental Margins, Geological Society of London, 17–18 September 2002.
- Dragoset, B., 1999, A practical approach to surface multiple attenuation, *The Leading Edge*, **18**(1), 104–108.
- Emsley D., Boswell, P. and Davis, P., 1998, Sub-basalt imaging using long offset reflection seismic data. 60<sup>th</sup> EAGE Conference, Expanded Abstracts, 1–48.
- Flidner, M.M., and White, R.S., 2001, Sub-basalt imaging in the Faeroe-Shetland Basin with large-offset data. *First Break* **19**, 247–252.
- Kjørboe, L., 1999, Stratigraphic relationships of the Lower Tertiary of the Faeroe Basalt Plateau and the Faeroe-Shetland Basin. *In: Fleet, A.J., & Boldy, S.A.R. (eds) Petroleum Geology of Northwest Europe: Proceedings of the 5<sup>th</sup> Conference*, 559–572, Geological Society of London.
- Lunnon, Z., Christie, P., and White, R., 2003, An evaluation of peak and bubble tuning in sub-basalt imaging: modelling and results. 65th Mtg. Eur. Assn. Geosci. Eng., paper C01.
- Mack, H., 1997, Seismic response of Tertiary basalt flows in the northeast Atlantic - a modelling study. 59th Mtg., Eur. Assn. Geosci. Eng., Session: B017.
- Martin, J., Ozbek, A., Combee, L., Lunde, N., Bittleston, S. and Kragh, E., 2000, Acquisition of marine point receiver seismic data with a towed streamer, 70th Ann. Internat. Mtg: Soc. of Expl. Geophys., 37–40.
- Morgan, J.V., Barton, P.J. and White, R.S., 1989, The Hatton Bank continental margin—III. Structure from wide-angle OBS and multichannel seismic refraction profiles. *Geophysical Journal International* **98**, 367–384.
- Planke, S., & Cambray, H., 1998, Seismic properties of flood basalts from Hole 917A downhole data, southeast Greenland volcanic margin. *In: Sanders, A.D., Larsen, H.C. and Wise, S.W. Jr., (eds) Proceedings of the Ocean Drilling Program, Scientific Results*, **152**, 453–462.
- Richardson, K.R., White, R.S., England, R.W., and Fruehn, J., 1999, Crustal structure east of the Faroe Islands, *Petroleum Geoscience* **5**, 161–172.
- Smallwood, J., 2002, The Marjun discovery: first oil in the Faroes, presented at: Frontier Exploration of

---

\*Mark of WesternGeco

Volcanic Continental Margins, Geological Society of London, 17–18 September 2002.

Smallwood, J.R. and White, R.S., 2002, Ridge-plume interaction in the North Atlantic and its influence on continental break-up and seafloor spreading. *In*: Jolley, D.W., and Bell, B.R. (eds), *The North Atlantic Igneous Province: stratigraphy, tectonic, volcanic and magmatic processes*, Special Publications **197**, 15–37, Geological Society, London.

White, R.S., 1997, Rift-plume interaction in the North Atlantic, *Philosophical Transactions of the Royal Society, London, Series A*, **355**, 319–339.

White, R.S., Fruehn, J., Richardson, K.R., Cullen, E., Kirk, W., Smallwood, J.R., and Latkiewicz, C., 1999, Faroes Large Aperture Research Experiment (FLARE): Imaging through basalts. *In*: Fleet, A.J., & Boldy, S.A.R. (eds) *Petroleum Geology of Northwest Europe: Proceedings of the 5<sup>th</sup> Conference*, 1243–1252, Geological Society, London.

White, N.J. and Lovell, B., 1997, Measuring the pulse of a plume with the sedimentary record. *Nature* **387**, 888–891.

White, R.S., Christie, P.A.F., Kusznir, N.J., Roberts, A., Hurst, N., Lunnion, Z., Parkin, C.J., Roberts, A.W., Smith, L.K., Spitzer, R., Surendra, A., and Tymms, V., 2002, iSIMM pushes frontiers of marine seismic acquisition. *First Break* **20**, 782–786.

Ziolkowski, A., Parkes, G., Hatton, L. and Haugland, T., 1982, The signature of an air-gun array - Computation from near-field measurements including interactions, *Geophysics* **47**, 1413–1421.

Ziolkowski, A., Hanssen, P., Gatliff, R., Li, X., and Jakubowicz, H., 2001, The use of low frequencies for sub-basalt imaging. 71st Ann. Internat. Mtg., Soc. Expl. Geophys., 74–77.

#### Acknowledgements

The authors wish to thank the Masters and crews of both the *RRS Discovery* and the *M/V Geco Topaz* for their expertise in acquiring high-quality datasets. We acknowledge Peter Sabel, Jon-Fredrik Hopperstad and Andy Harber of WesternGeco for valuable support during the pre-survey modelling. John Bacon and colleagues in the WesternGeco data processing group have brought experience and insight to the data analysis. iSIMM is supported by Liverpool and Cambridge Universities, Schlumberger Cambridge Research, Badley Geoscience Limited, WesternGeco, Amerada Hess, Anadarko, BP, ConocoPhillips, ENI UK, Statoil, Shell, the Natural Environment Research Council and the Department of Trade and Industry. However, the views expressed here are those of the authors who are solely responsible for any errors.